https://doi.org/10.5194/egusphere-2025-537
Preprint. Discussion started: 17 March 2025

Technical note: Towards a stronger observational support for haze pollution control by interpreting carbonaceous aerosol results derived from different measurement approaches

Yuan Cheng, Ying-jie Zhong, Zhi-qing Zhang, Xu-bing Cao, Jiu-meng Liu*

State Key Laboratory of Urban Water Resource and Environment, School of Environment, Harbin Institute of Technology, Harbin, 150090, China

* Corresponding author. Jiu-meng Liu (jiumengliu@hit.edu.cn).

Abstract

As China's fine particulate matter ($PM_{2.5}$) has decreased nationwide during the last decade, further improvement of air quality became more challenging, imposing higher requirements on the observational support for the understanding of aerosol sources. This was particularly the case for the severe cold climate region in Northeast China, which suffered from relatively slow decreasing rate and high exposure risk of $PM_{2.5}$. Here we evaluated carbonaceous aerosol data measured by different sampling and analytical approaches, based on field campaigns conducted during a frigid winter and an agricultural-fire impacted spring in Harbin. For both the high- and low-volume sampling, a total of four sets of organic and elemental carbon results were derived by applying two commonly-used temperature protocols (IMPROVE-A, i.e., IMPV, and NIOSH) to both untreated filters and those extracted by methanol. Only the IMPV-based results measured before the extraction were found to be indicative of aerosol sources, e.g., in reasonable accordance with secondary aerosol formation in winter and open burning impacts in spring. Thus the analytical method of IMPROVE-A on untreated samples was recommended for future field observations and source apportionments of $PM_{2.5}$ in the studied region. In addition, although the low- and high-volume samplers typically led to comparable measurement results for various species, exceptions were identified for water-soluble potassium (K^+) and some fire-emitted chromophores. We suggested that K^+ detected by

https://doi.org/10.5194/egusphere-2025-537
Preprint. Discussion started: 17 March 2025

different $PM_{2.5}$ samplers may not be directly comparable, and K^+ should be used with caution as a biomass burning tracer for studies relying on high-volume measurements.

https://doi.org/10.5194/egusphere-2025-537
Preprint. Discussion started: 17 March 2025

1. Introduction

Carbonaceous aerosols are a complex mixture of compounds exhibiting a gradual change in chemical and physical properties (Pöschl, 2005; Andreae and Gelencsér, 2006), e.g., from colorless organics with low molecular weights, to "dark" brown carbon with relatively high thermal stabilities (Chakrabarty et al., 2023), and finally to refractory black carbon which is strongly light-absorbing. As important contributors to both fine particulate matter ($PM_{2.5}$) pollution and radiative forcing, they have long been targeted to achieve a synergistic improvement of air quality and mitigation of climate change (Fuzzi et al., 2015; von Schneidemesser et al., 2015; Liu et al., 2022). However, it remains a challenge to properly represent carbonaceous aerosols in chemical transport models, as each step along the way between the estimations of sources and tempo-spatial variations is difficult. For example, considerable uncertainties exist in the open burning emission, secondary organic aerosol (SOA) budget and black carbon lifetime (Andela et al., 2022; Chang et al., 2022; Zhong et al., 2023). This in turn introduces substantial uncertainties to the climate and health effects of carbonaceous aerosols (Li et al., 2022).

Field observational data on carbonaceous aerosols, including those derived from ground and aircraft measurements, are essential to constrain the simulation results and subsequently to improve the model performance (Philip et al., 2014; Wang et al., 2014b, 2018; Gao et al., 2022; Eckhardt et al., 2023). Relying on on-line instruments such as the Single Particle Soot Photometer (SP2), aircraft studies typically covered relatively short periods (e.g., up to about one month) but provided measurement results with high time and spatial resolutions (Samset et al., 2014). Offline and semi-continuous techniques (e.g., lab and field carbon analyzers for elemental carbon) were more commonly used in ground observations, giving rise to datasets with relatively low time resolutions

https://doi.org/10.5194/egusphere-2025-537
Preprint. Discussion started: 17 March 2025

but spanning several months to decades (Dao et al., 2019; Hand et al., 2024). After accounting for the difference in time resolution, the integration of carbonaceous aerosol data across studies and regions was still not straightforward. A major obstacle was caused by the multitude of measurement principles (Petzold et al., 2013), which was intensively reflected by the considerable and, more importantly, variable discrepancies in black carbon results among different methods (Buffaloe et al., 2014; Li et al., 2019; Pileci et al., 2021; Tinorua et al., 2024). This problem was far from being properly addressed, although great efforts have been devoted to refine the respective measurement approach such as the thermal-optical (Cavalli et al., 2010), optical (Collaud Coen et al., 2010) and SP2 (Laborde et al., 2012) techniques. In addition, this problem was to some extent overlooked in China, which might be partially responsible for the inconsistent source apportionment results obtained by different studies. For example, both Zheng et al. (2015) and Liu et al. (2020) applied the EC-tracer method to estimate secondary OC (SOC) during winter in Beijing, but the two studies derived conflicted conclusions on the contribution of heterogeneous chemistry to SOC formation (i.e., minimal vs. significant) since different analytical methods for EC were deployed. Such inconsistencies substantially weakened the observational support for the understanding of aerosol sources and thus the control of haze pollution.

With a considerable decrease in the national $PM_{2.5}$ since 2013, it became more challenging to further improve the air quality in China (Cheng et al., 2021). This imposed higher requirements on the observational insights into aerosol sources, including the evaluation of carbonaceous aerosol results among various measurement approaches. Here we focused on the widely-used thermal-optical method, which separates carbonaceous components into two fractions with different thermal stabilities and light absorption capacities, i.e., organic carbon (OC) and elemental carbon (EC). The

https://doi.org/10.5194/egusphere-2025-537
Preprint. Discussion started: 17 March 2025

basis of the separation includes two points: EC survives to higher temperatures than OC, and the removal of EC leads to a rapid increase in the filter transmittance and reflectance signals. A major problem in this method is that a considerable fraction of OC could be transformed into char-OC, which is difficult to be robustly distinguished from EC with respect to either thermal or optical behavior. In addition, the amount and optical properties of char-OC were found to depend on the temperature protocol deployed (Yu et al., 2002; Yang and Yu, 2002; Subramanian et al., 2006). This to a large extent explained the EC discrepancies among various protocols. However, it remained unclear how the charring process and thus the EC measurement were influenced by OC sources and composition (Chiappini et al., 2014). In addition, to reduce or minimize the interference from char-OC, several investigators have tried to remove a fraction of OC from the samples before thermal-optical analysis, by extracting the filters using water, methanol or other solvents (Piazzalunga et al., 2011; Giannoni et al., 2016; Lappi and Ristimäki, 2017; Aakko-Saksa et al., 2018; Hu et al., 2023). However, inconsistent patterns were identified for the effects of OC removal on EC determination, with evidences available for both an increase (e.g., Piazzalunga et al., 2011) and a decrease in EC (e.g., Hu et al., 2023) after the extraction. The discussions above indicated that the thermal-optical methods, including the practicability of sample pretreatment by extraction, merit further investigations.

In this study, we compared carbonaceous aerosol results determined by different analytical as well as sampling approaches, based on filter samples collected in Harbin, the northernmost megacity in China. Compared to other megacities such as Beijing, Harbin is characterized by the frigid winter (with an average temperature of about –20 °C in January) and the massive agricultural sector in surrounding areas (i.e., the Songnen Plain in Northeast China). In addition, Harbin and other cities

https://doi.org/10.5194/egusphere-2025-537
Preprint. Discussion started: 17 March 2025

in Northeast China have largely been overlooked in clean air actions and thus studies on haze, as indicated by the limited observational data available (Liu et al., 2022). This lack of investigation was partially responsible for the relatively slow decreasing rate (Xiao et al., 2022) and high exposure risk (Wei et al., 2023) of $PM_{2.5}$ in this distinct region. Thus our study on measurement methods of carbonaceous aerosols is expected to be a support for future efforts on exploration of the $PM_{2.5}$ sources in Northeast China, which are essential for further improving the regional air quality.

2. Methods

2.1 Field sampling

$PM_{2.5}$ samples were collected at an urban site in Harbin, i.e., on the campus of Harbin Institute of Technology (HIT), during the winter and spring of 2021. The sampling was done by a mass flow controlled high-volume sampler (TE-6070BLX-2.5-HVS; Tisch Environmental, Inc., OH, USA) and a low-volume sampler (MiniVol; Airmetrics, OR, USA), operated using quartz-fiber filters (Pall Corporation, NY, USA) at flow rates of 1.13 m^3/min and 5 L/min, respectively. The flow rates, together with the particle-laden filter areas, could be translated into the face velocities of 46.34 and 7.35 cm/s for the high- and low-volume (HV and LV) samplers, respectively. This indicated that when the two samplers were run in parallel, the HV-to-LV ratio of particle loading would be 6.3.

The 2021 winter campaign covered the entirety of January, the coldest month during that year with an average temperature of –19 °C, whereas the spring campaign was conducted during 10–30 April of 2021, a period with frequent occurrences of agricultural fires (as indicated by the satellite-based active fire detection results; Figure S1). For both seasons, the HV sampler was used to collect daytime (09:00–16:00) and nighttime (21:00–05:00 of the next day) samples, while the LV one was operated on a daily basis, leading to 24-h integrated samples. Each LV sample generally

https://doi.org/10.5194/egusphere-2025-537
Preprint. Discussion started: 17 March 2025

corresponded to two HV samples, although the two samplers were not exactly parallel. One reason for the relatively short sampling durations of HV was to avoid extremely high particle loadings which could make the filters unsuitable for thermal-optical analysis (Lappi and Ristimäki, 2017).

2.2 Laboratory analysis

For both the HV and LV samples, two punches were prepared to determine OC and EC using a thermal-optical carbon analyzer (DRI-2001; Atmoslytic Inc., CA, USA). One punch was directly measured, while the other one was immersed in methanol (HPLC grade; Fisher Scientific Company L.L.C., NJ, USA) for an hour without stirring or sonication, dried in air for another hour, and then analyzed. All the pairs of untreated and extracted punches were measured using the IMPROVE-A and NIOSH temperature protocols, both of which were operated with transmittance charring correction. Inter-protocol comparisons showed good repeatability for both the total carbon (TC) and optical attenuation (ATN) results (Figure 1), demonstrating the robustness of the analyzer for detecting carbon and filter transmittance signals (I). Here ATN was calculated as $\ln(I_{final}/I_{initial})$, where $I_{initial}$ and I_{final} indicate I measured at beginning (i.e., when the particle-laden filter has not been heated) and end (i.e., when all the deposited carbon has been combusted off the filter) of thermal-optical analysis, respectively. ATN was of interest because it was closely related to EC loading (EC_s, in $\mu g/cm^2$), e.g., with a linear dependence for relatively low EC_s levels (Chen et al., 2020; Liu et al., 2020).

In addition, following the method developed by Hecobian et al. (2010), wavelength-resolved light absorption coefficients (b_{abs}) of the methanol extracts, i.e., the dissolved brown carbon (BrC), were measured using a spectrophotometer (Ocean Optics Inc., FL, USA) coupled with a 2.5-m long liquid waveguide capillary cell (LWCC; World Precision Instruments, FL, USA). Inorganic ions and

https://doi.org/10.5194/egusphere-2025-537
Preprint. Discussion started: 17 March 2025

levoglucosan were also determined for the HV and HV samples, by analyzing their water extracts using a Dionex ion chromatography system (ICS-5000$^+$; Thermo Fisher Scientific Inc., MA, USA).

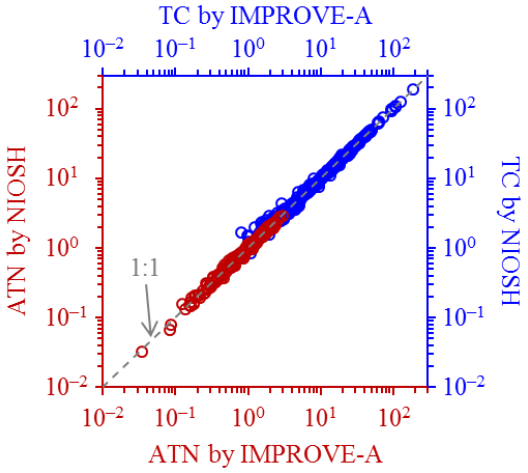

Figure 1. Comparisons of TC (in μgC/cm^2) and ATN (dimensionless) measured using different temperature protocols. Results from the HV and LV samples, both untreated and extracted, were combined for the comparisons. Linear regression of the NIOSH-based ATN on that determined by IMPROVE-A led to a slope of 0.99 ± 0.00 (r = 1.00; intercept was set as zero). Similar regression results (i.e., slope = 0.99 ± 0.00; r = 1.00) were obtained for TC. The good repeatabilities on one hand demonstrated the performance of carbon analyzer for measuring the carbon and laser transmittance signals, and on other hand indicated a homogeneous distribution of carbonaceous components for not only the untreated but also the extracted filters, i.e., a negligible disturbance of EC as well as other insoluble carbon by the extraction.

2.3 Open-access data

Meteorological data (e.g., temperature and relative humidity) and air quality data (e.g., $PM_{2.5}$, PM_{10} and CO) for the measurement periods were obtained with a time resolution of 1 h from Weather Underground (https://www.wunderground.com/) and the China National Environmental Monitoring Center (CNEMC; https://air.cnemc.cn:18007/), respectively.

3. Results and discussion

3.1 Evaluation of EC results from the winter campaign

https://doi.org/10.5194/egusphere-2025-537
Preprint. Discussion started: 17 March 2025

A precondition for proper separation of OC and EC is that the filter transmittance signal (*I*) could properly reflect the formation of light-absorbing char-OC during the inert mode (which would result in a decrease in *I*), and the combustion, i.e., removal, of char-OC and EC during the oxidation mode (which would result in an increase in *I*). An empirical approach to evaluate this precondition is to examine the dependence of ATN on EC_s (Subramanian et al., 2006). A linear relationship was typically observed for relatively low EC_s levels and in this case, the precondition was commonly believed to be valid. However, the linearity did not necessarily extend when EC_s further increased, since previous studies frequently found that the measured ATN could be considerably lower than expected for heavily-loaded samples (Shen et al., 2013; Costa et al., 2016; Chen et al., 2020). The deviation of ATN vs. EC_s dependence from linear relationship was usually termed the loading effect, and a traditional explanation was that ATN became less sensitive to the variation of EC_s as filter loading increased. An extreme case was observed during winter in Beijing, that the ATN values were largely unchanged for heavily-loaded filters with TC varying between 150 and 300 $\mu gC/cm^2$ (Liu et al., 2019). For the samples showing non-linear ATN vs. EC_s dependence, their EC results should be interpreted with caution.

We first investigated the relationship between ATN and EC_s for the wintertime HV samples, focusing on the results from IMPROVE-A. For the untreated filters, ATN correlated linearly with EC_s (leading to a regression slope of 42.8 $\pm$ 1.9 m^2/gC and a close-to-zero intercept; r = 0.95) when the filters were lightly to moderately loaded, i.e., when the EC_s levels were below 5 $\mu gC/cm^2$ (Figure 2a). The physical meaning of the slope was the mass absorption efficiency (MAE) of black carbon, but with artifacts such as that caused by the multiple scattering effect (Lack et al., 2014). The overall impact of various artifacts results in an overestimation of MAE, typically by factors of ~3 (Knox et

https://doi.org/10.5194/egusphere-2025-537
Preprint. Discussion started: 17 March 2025

al., 2009; Qin et al., 2018). The linearity determined for the EC_s range of below 5 μgC/cm^2 did not hold for the more heavily loaded samples (N = 3, as highlighted by the solid circles in Figure 2a), showing evidence for the loading effect. For the extracted samples, a linear correlation between ATN and EC_s was also identified for relatively low EC loadings (Figure 2b), with a similar relationship (i.e., a regression slope of 41.5 m^2/gC and a close-to-zero intercept; r = 0.95) to that derived from the untreated filters. However, it was noteworthy that EC_{max}, the upper limit of EC loading for a linear ATN vs. EC_s dependence, was only 3 μgC/cm^2 for the extracted filters, much lower than that determined for the untreated ones. Due to the shift of EC_{max}, 51% of the extracted samples showed evidence for the loading effect, whereas this fraction was only 5% before extraction.

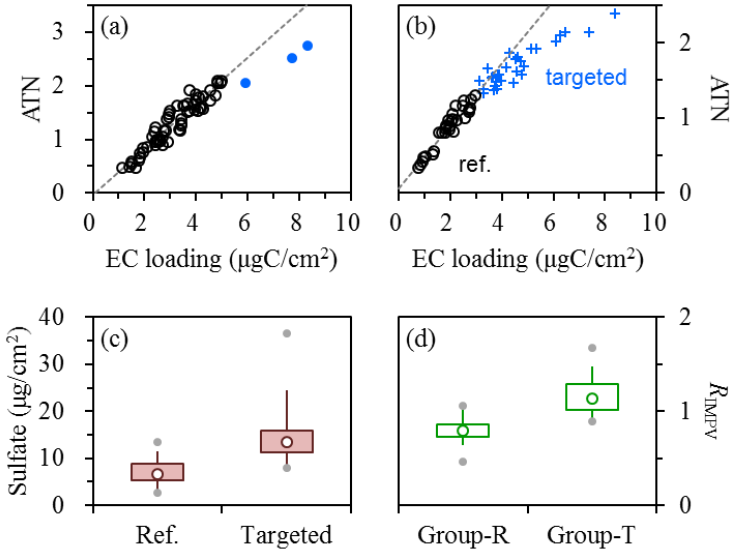

Figure 2. Relationships between ATN and EC loading, i.e., EC_s, for the **(a)** untreated and **(b)** extracted HV filters collected in winter, using the IMPROVE-A protocol. Linear dependences were observed for the untreated samples with EC_s below 5 μgC/cm^2 and for the extracted samples with EC_s below 3 gC/cm^2, as indicated by the dashed lines in (a) and (b), respectively. In (b), the extracted filters showing non-linear ATN vs. EC_s dependence were termed as the targeted samples; correspondingly, the others were referred to as the reference ones. **(c)** Comparison of sulfate loadings between the reference and targeted samples. **(d)** Comparison of the $EC_{extracted}$ to $EC_{untreated}$ ratios, i.e., R_{IMPV}, between the reference and targeted groups of wintertime HV samples (labelled as

https://doi.org/10.5194/egusphere-2025-537
Preprint. Discussion started: 17 March 2025

and Group-T, respectively). The targeted group indicated the targeted filters and the corresponding untreated ones, while the reference group indicated the remaining pairs. Lower and upper box bounds indicate the 25th and 75th percentiles, the whiskers below and above the box indicate the 5th and 95th percentiles, the solid circles below and above the box indicate the minimum and maximum, and the open circle within the box marks the median. All the EC results involved were measured by IMPROVE-A.

The discussions above raised a question that why the extraction significantly reduced EC_{max} for the HV samples. In principle, two factors could be responsible for the non-linear dependence of ATN on EC_s, including gradual saturation of ATN with increasing filter loading (the traditional explanation; Subramanian et al., 2006) and overestimation of EC mass. The EC_{max} of untreated samples corresponded to an ATN of 2.1, indicating that the saturation was presumably not a concern for the ATN results below this value. Regarding the extracted samples showing evidence for the loading effect (i.e., the targeted samples), ATN stayed below 2.1 for nearly all of them (28 out of 31), thus their non-linear ATN vs. EC_s dependences should be primarily attributed to the overestimation of EC mass rather than the saturation of ATN. Compared to the other extracted samples, the targeted ones were characterized by substantially higher sulfate loadings (Figure 2c). It was inferred that in addition to EC, the abundant sulfate was also a non-negligible contributor to ATN (e.g., through backward scattering; Petzold et al., 2005; Collaud Coen et al., 2010). Thus when these samples were heated in the carbon analyzer, volatilization of sulfate would lead to a decrease in ATN, i.e., an increase in filter transmittance signal. This was expected to result in a premature split of OC and EC, and eventually an overestimation of EC. Other scattering components such as nitrate and secondary organic aerosol (SOA) were not considered here, since they were soluble in methanol and should be absent in the extracted filters.

Comparison of EC between the targeted samples and the corresponding untreated ones (i.e., the targeted group) showed an overall increasing trend after the extraction (Figure 2d). For these

https://doi.org/10.5194/egusphere-2025-537
Preprint. Discussion started: 17 March 2025

pairs of wintertime HV filters, the ratio of $EC_{extracted}$ (i.e., EC measured in the extracted samples) to $EC_{untreated}$ (i.e., EC measured in the untreated samples) averaged 1.16 ±0.20. The extraction-induced increase in EC coincided with the overestimation of elemental carbon mass by $EC_{extracted}$, which was inferred to be associated with the presence of abundant sulfate in the extracted filters.

For the other pairs of wintertime HV samples (i.e., the reference group), the $EC_{extracted}$ to $EC_{untreated}$ ratios averaged 0.80 ±0.12, pointing to a decrease in EC after the extraction (Figure 2d). This was also the case for all the LV samples collected during the winter campaign, with comparable $EC_{extracted}$ to $EC_{untreated}$ ratios (averaging 0.78 ± 0.12). Here the LV samples were not divided into subgroups because non-linear dependence of ATN on EC_s was identified neither before nor after the extraction (Figure S2). Given that the loss of insoluble carbon (e.g., EC) was negligible for our extraction procedures (Figure 1 and Cheng et al., 2024), the extraction-induced decrease of EC likely pointed to the underestimation of elemental carbon mass by $EC_{extracted}$. A common feature for the HV samples in the reference group and the entirety of the LV samples was the relatively low sulfate loadings. Cheng et al. (2024) inferred that small amounts of sulfate likely favored the transmission of light through the extracted filters (e.g., by forward scattering; Petzold et al., 2005; Collaud Coen et al., 2010). In this case, when the extracted samples were heated during thermal-optical analysis, volatilization of sulfate would induce a drop of filter transmittance signal, which could not be distinguished from that caused by the formation of char-OC. This was expected to result in an overcorrection for char-OC, i.e., an underestimation of EC.

The contrasting $EC_{extracted}$ to $EC_{untreated}$ ratios observed for the two groups of wintertime HV samples suggested that the influence of sulfate on the transmittance signal of the extracted filter was likely loading-dependent. The influence was inferred to be dominated by forward scattering when

https://doi.org/10.5194/egusphere-2025-537
Preprint. Discussion started: 17 March 2025

sulfate was less abundant (e.g., for the reference group), whereas by backward scattering with relatively high sulfate loadings (e.g., for the targeted group). The $EC_{extracted}$ results appeared to be biased by different artifacts in these two cases, resulting in underestimations or overestimations of elemental carbon mass, respectively. The sulfate-induced artifacts for $EC_{extracted}$ could be more directly reflected by the positive dependence of the $EC_{extracted}$ to $EC_{untreated}$ ratio on sulfate loading. As shown in Figure 3, the turning point for the artifact shifting from an underestimation to overestimation of elemental carbon mass by $EC_{extracted}$ occurred in the sulfate loading range of 10–15 μg/cm^2. Figure 3 also suggested that the artifacts for $EC_{extracted}$ were difficult to be accounted for, e.g., by a constant correction factor. This prohibited the use of $EC_{extracted}$ for further analysis of aerosol composition and sources.

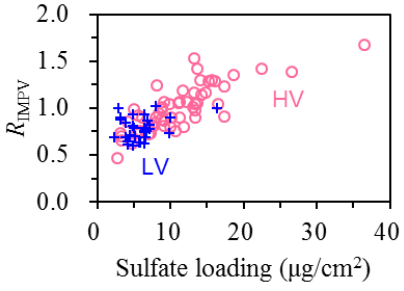

Figure 3. Dependence of R_{IMPV}, i.e., the $EC_{extracted}$ to $EC_{untreated}$ ratio determined by IMPROVE-A, on sulfate loading in winter. Consistent trends were observed by the HV and LV samples. The relatively wide range of R_{IMPV} (approximately 0.5–1.5) provided solid evidence for the invalidation of the $EC_{extracted}$ to $EC_{untreated}$ ratio as an indicator for the extraction-induced loss of EC.

For the untreated filters, ATN exhibited a strong linear correlation with EC_s for both HV and LV, with three heavily-loaded HV samples as the only exception. Actually, for the three samples, their ATN vs. EC_s relationships did not deviate markedly from the regression line determined for the lower EC_s loadings. Therefore, we suggested that when applying IMPROVE-A to the winter samples, the measurement uncertainties should be less significant for $EC_{untreated}$ compared to

https://doi.org/10.5194/egusphere-2025-537
Preprint. Discussion started: 17 March 2025

$EC_{extracted}$.

The same conclusion could be reached by interpreting the OC to EC ratios (OC/EC). It has been widely accepted that OC/EC depended strongly on SOA formation, after excluding the distinct events impacted by irregular emissions such as fireworks and open burning. Such events were not evident throughout the winter campaign, and thus OC/EC was expected to increase with the enhancement of secondary aerosol production. Here we used the relative abundance of secondary inorganic ions (sulfate, nitrate and ammonium, i.e., SNA) compared to carbon monoxide (a typical primary species), i.e., the SNA/CO ratio, as an indicator for the significance of secondary aerosols. A benefit of using SNA/CO was that it was independent of EC measurement. The OC/EC ratio corresponding to $EC_{untreated}$ [i.e., $(OC/EC)^{*}$] was determined directly by the thermal-optical results from the untreated samples. For $EC_{extracted}$, the corresponding OC/EC [i.e., $(OC/EC)^{\#}$] was calculated as $(TC_{untreated} - EC_{extracted})/ EC_{extracted}$, where $TC_{untreated}$ indicates the total carbon concentration measured before the extraction. As shown in Figure 4 for the wintertime HV samples, $(OC/EC)^{*}$ exhibited reasonable accordance with SNA/CO (r = 0.72) but $(OC/EC)^{\#}$ did not (r = 0.02). The clear association between $(OC/EC)^{*}$ and SNA/CO, which was also supported by the results from LV (r = 0.66; Figure S3), provided additional evidence for the robustness of $EC_{untreated}$ determined by IMPROVE-A.

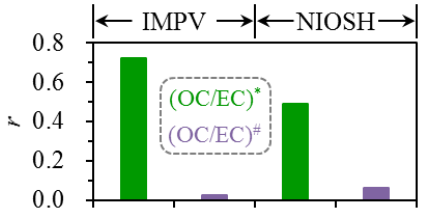

Figure 4. Comparison of r values derived from the linear regressions of various OC/EC estimations on SNA/CO, based on the wintertime HV samples. IMPV indicates the IMPROVE-A temperature

https://doi.org/10.5194/egusphere-2025-537
Preprint. Discussion started: 17 March 2025

protocol. A total of four sets of OC/EC ratios were determined using different protocols and pre-treatment approaches. The OC/EC ratio measured by the untreated samples using IMPROVE-A, i.e., the IMPV-based $(OC/EC)^{*}$, exhibited the strongest association with SNA/CO.

Compared to IMPROVE-A, NIOSH led to weaker correlations between $(OC/EC)^{*}$ and SNA/CO, as indicated by the smaller r values determined (0.49 vs. 0.72 for HV and 0.18 vs. 0.66 for LV; Figures 4 and S3). In addition, the NIOSH-based $(OC/EC)^{\#}$ did not exhibit apparent dependence on SNA/CO either (r = 0.06 and 0.34 for HV and LV, respectively). Thus Figures 4 and S3 clearly reflected the limitations of NIOSH-based OC/EC and thus NIOSH-based EC, further highlighting the benefit of using $EC_{untreated}$ determined by IMPROVE-A.

3.2 Evaluation of EC results from the spring campaign

In this section we evaluated the EC results from April, also starting with the HV samples analyzed by IMPROVE-A. To highlight the role of agricultural fires, we first separated the April samples into two groups (namely the fire-impacted and typical samples), which were characterized by considerable and insignificant impacts of open burning, respectively. As described in Supporting Information, the criteria for fire-impacted samples could be simplified as a levoglucosan to $TC_{untreated}$ ratio (f_{LG}; on a basis of carbon mass) of above 1.8%, based on a synthesis of f_{LG}, the levoglucosan to water-soluble potassium ratio (LG/K^{+}) and satellite-based fire hotspots (Figure S4). Before filter extraction, the dependence of ATN on EC_s could be approximated by a liner function (with a slope of 33.4 $\pm$1.5 m^2/gC and a close-to-zero intercept; r = 0.97) for all the typical samples and the majority of the fire-impacted ones (Figure 5a), leading to an EC_{max} of 8 $\mu gC/cm^2$. For three of the fire-impacted samples, EC_s exceeded this threshold value and the ATN vs. EC_s relationships were found to deviate significantly from the regression line, especially for the two samples with EC_s above 10 $\mu gC/cm^2$ (as highlighted in Figure 5a).

https://doi.org/10.5194/egusphere-2025-537
Preprint. Discussion started: 17 March 2025

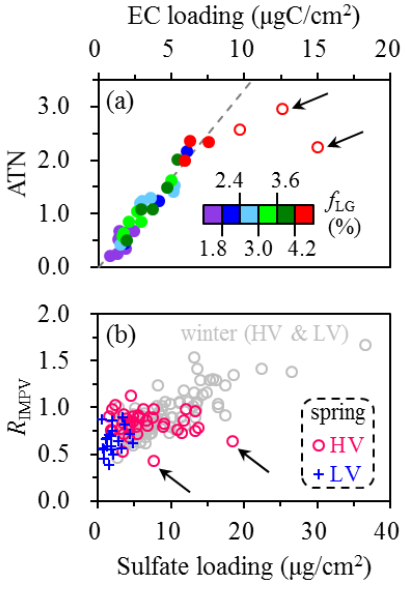

Figure 5. (a) Dependence of ATN on EC loading (EC_s) for the untreated HV samples collected in spring, color-coded by f_{LG} levels. Samples with linear and non-linear ATN vs. EC_s dependence are shown by the solid and open circles, respectively. f_{LG} values higher than 1.8% indicated significant impacts of agricultural fires. **(b)** Dependence of R_{IMPV}, i.e., the $EC_{extracted}$ to $EC_{untreated}$ ratio, on sulfate loading in spring. Results from winter were also shown for comparison. In general, a consistent relationship was observed between R_{IMPV} and sulfate loading for the samples, including both HV and LV, from different seasons. The only exceptions were two HV samples collected in spring, as highlighted by the arrows. The two distinct samples were also highlighted in (a), corresponding to the two points showing significant non-linear dependences of ATN on EC loading. All the EC results involved were measured by IMPROVE-A.

To elucidate factors responsible for the observed non-linear dependence of ATN on EC_s, we compared EC results from the untreated and extracted filters. Given the relatively low sulfate loadings observed throughout April (Figure 5b), it was with expectation that EC generally decreased after the extraction. After excluding two distinct samples, the $EC_{extracted}$ to $EC_{untreated}$ ratios averaged 0.84 ± 0.11, comparable to results from the reference group in winter. The two distinct samples, which were collected on the nights of April 10 and 20, 2021, showed $EC_{extracted}$ to $EC_{untreated}$ ratios of as low as 0.64 and 0.43, respectively. Such significant extraction-induced decreases in EC could hardly be explained by the interference from sulfate in thermal-optical analysis of the extracted

https://doi.org/10.5194/egusphere-2025-537
Preprint. Discussion started: 17 March 2025

filters (Figure 5b). Instead, the two distinct samples were found to show several noteworthy features: (i) they corresponded to the two samples showing significant non-linear ATN vs. EC_s dependences before the extraction (Figure 5a); (ii) their f_{LG} levels were at the higher end of the fire-impacted samples (with levoglucosan concentrations exceeding 7 μg/m^3), indicating extremely strong impacts of open burning (Figure 5a); (iii) their LG/K^+ ratios (> 1.7) were also at the higher end of the fire-impacted samples, which were characteristic of the emissions from smoldering combustion (Gao et al., 2003; Sullivan et al., 2019); (iv) their ATN decreased apparently after the extraction, by ~1.0 which were about one order of magnitude higher than results from the typical samples (~0.1). Thus it was inferred that $EC_{untreated}$ of the distinct samples likely involved some light-absorbing organic compounds (i.e., BrC) emitted by agricultural fires with relatively low combustion efficiencies, and the absorption capacities of these organics were strong enough to make them a considerable contributor to ATN measured at 632 nm. Indeed, the BrC-related overestimation of elemental carbon mass was expected to be reduced considerably after the extraction. However, such overestimation seemed apparent only for the two distinct samples (Figure 5a). In addition, recalling the lower-than-one $EC_{extracted}$ to $EC_{untreated}$ ratios observed for the other April samples (i.e., the sulfate-related artifact raised for the extracted filters), the methanol extraction actually brought little benefit for the determination of EC by IMPROVE-A.

Unlike HV, all the LV samples showed a consistent relationship between ATN and EC_s before the extraction (Figure S5). It appeared that the strongly absorbing organics that could interfere EC measurement were mainly concentrated in some agriculture-fire smoke emitted at night (as indicated by the two distinct HV samples), whereas their influence on EC determination was considerably weakened for the 24-h integrated LV samples. Thus the linear ATN vs. EC_s dependence,

https://doi.org/10.5194/egusphere-2025-537
Preprint. Discussion started: 17 March 2025

which was valid for all the untreated LV samples analyzed by IMPROVE-A, provided little evidence for the necessity of methanol extraction.

We also investigated the OC/EC vs. f_{LG} relationship for the HV samples collected in April. Open burning was considered to be favorable for the increase of ambient OC/EC, since the aerosols emitted were frequently found to be almost entirely organic (Liu et al., 2016; Garofalo et al., 2019; Gkatzelis et al., 2024). Then it was not surprising to observe a moderate correlation between $(OC/EC)^*$ and f_{LG} (r = 0.59; Figure 6), i.e., an increasing trend of $(OC/EC)^*$ with stronger impacts of agricultural fires. In addition, $(OC/EC)^*$ also depended moderately on SNA/CO (r = 0.49; Figure 6). This was with expectation as well, given the observational evidence on the concurrent enhancements of secondary inorganic and organic aerosols (e.g., Liu et al., 2020; Cheng et al., 2022). Replacing $(OC/EC)^*$ with $(OC/EC)^\#$ did not effectively strengthen the association of OC/EC with f_{LG} or SNA/CO (Figure 6). This conclusion also held for the LV samples (Figure 6). In summary, we did not observe additional evidence supporting the incorporation of methanol extraction with IMPROVE-A.

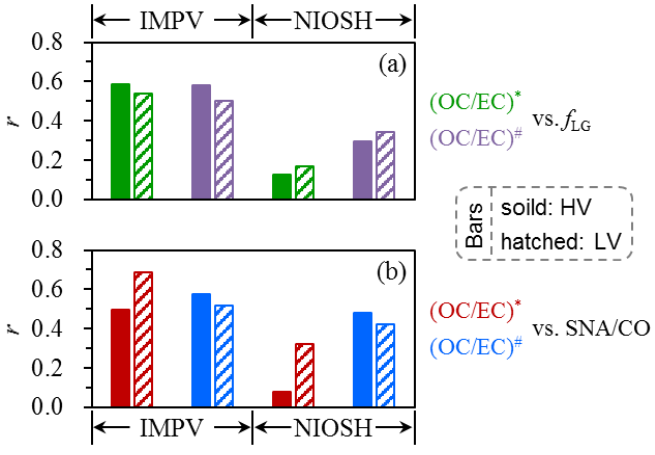

Figure 6. Comparisons of r values derived from the linear regressions of various OC/EC estimations

https://doi.org/10.5194/egusphere-2025-537
Preprint. Discussion started: 17 March 2025

on **(a)** f_{LG} and **(b)** SNA/CO, based on the spring samples. IMPV indicates the IMPROVE-A temperature protocol. Results from the HV and LV filters are shown by solid and hatched bars, respectively. For both HV and LV, a total of four sets of OC/EC ratios were determined using different protocols and pre-treatment approaches. In general, OC/EC ratios measured by the untreated samples using IMPROVE-A, i.e., the IMPV-based $(OC/EC)^*$, exhibited reasonable associations with aerosol sources. Using other OC/EC estimations failed to or did not effectively enhance the associations.

Compared to $(OC/EC)^*$ determined by IMPROVE-A, the NIOSH-based $(OC/EC)^*$ and $(OC/EC)^\#$ were less indicative of aerosol sources which could be reflected by f_{LG} and SNA/CO. This was the case for both the HV and LV samples (Figure 6). Based on the discussions above, $EC_{untreated}$ determined by IMPROVE-A (EC^*) was also recommended for the conditions with prevalence of agricultural fires (i.e., April), in line with the conclusion derived for winter. In addition, it should be kept in mind that EC^* could overestimate elemental carbon mass due to the interference from strongly absorbing BrC. However, such overestimation was generally uncommon, i.e., was considerable only for some nighttime samples under extremely strong influences of low-efficiency agricultural fires (as indicated by the two distinct HV samples; Figure 5).

3.3 Comparison of measurement results from the HV and LV samplers

As mentioned in the Methods section, each LV sample corresponded to a pair of daytime and nighttime HV samples, indicating that measurement results from the HV samples could be averaged and then compared to those determined by LV. Here the inter-sampler comparison was performed for several components that are of broad interest in field observations, including elemental and organic carbon, secondary inorganic ions (sulfate, nitrate and ammonium), other water-soluble ions (potassium and chloride), organic tracer for biomass burning (levoglucosan), BrC mass concentration and light absorption coefficient. Based on the evaluation results in previous sections, EC^* and the corresponding OC, i.e., OC^* (measured before the extraction using IMPROVE-A), were

https://doi.org/10.5194/egusphere-2025-537
Preprint. Discussion started: 17 March 2025

selected for the comparison. In addition, following Cheng et al. (2024), BrC mass was calculated as the difference in TC between the untreated and extracted filters, while BrC absorption was investigated at a wavelength of 365 nm, i.e., $(b_{abs})_{365}$.

As shown in Figure 7, the two samplers generally led to comparable measurement results for all the species investigated. For example, the LV-to-HV ratios typically fell within the range of 0.8–1.2, i.e., results from the two samples generally agreed within ±20%. However, it was noticed that K^+ was the only component with the majority of the LV results lower than HV. In addition, the LV-to-HV ratio of K^+ was found to depend positively on the ratio of $PM_{2.5}$ to PM_{10} (Figure 8a). The $PM_{2.5}$ to PM_{10} ratio was strongly associated with the influence of dust, typically exhibiting a decreasing trend as the impact of dust became stronger (Putaud et al., 2010). Thus the events with decreased LV-to-HV ratios of K^+ presumably coincided with dust episodes, when relatively large particles were expected to be a non-negligible contributor to K^+ (Wang et al., 2014a). Then a likely cause for the dependence shown in Figure 8a was that the impactor performances (e.g., the size-cut curves) were different for the two samplers, such that some relatively large particles, if present, could be collected onto the HV filter but would be removed by the impactor of LV.

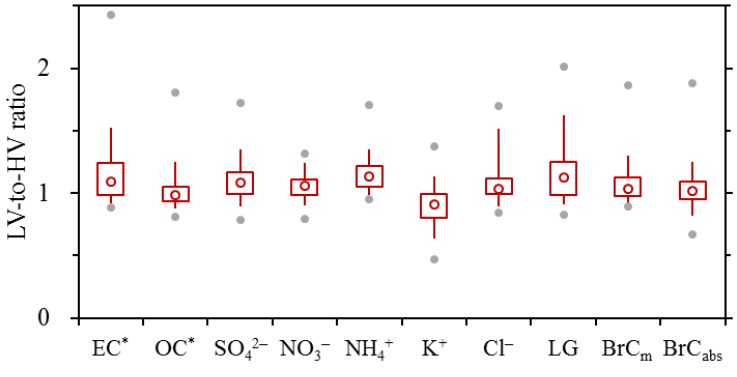

Figure 7. The LV-to-HV ratios determined for various species. BrC_m and BrC_{abs} indicate the mass

https://doi.org/10.5194/egusphere-2025-537
Preprint. Discussion started: 17 March 2025

404 concentration and $(b_{abs})_{365}$ of brown carbon, respectively.

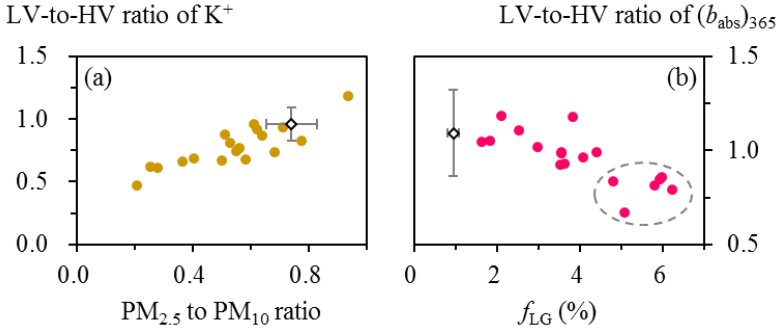

405

406 **Figure 8**. **(a)** Dependence of the LV-to-HV ratio of K^+ on the $PM_{2.5}$ to PM_{10} ratio. **(b)** Dependence
407 of the LV-to-HV ratio of $(b_{abs})_{365}$ on f_{LG}. Results from spring are shown on a sample-by-sample basis,
408 as indicated by the solid circles. For winter, only the average results are shown as indicated by the
409 diamonds. In (b), the events with substantially lower LV-to-HV ratios of $(b_{abs})_{365}$ are highlighted by
410 the dashed oval.

411 In addition, it was noticed that although the two samplers led to generally comparable $(b_{abs})_{365}$
412 results, the corresponding LV-to-HV ratios decreased substantially (e.g., down to 0.67) for the
413 episodes with extremely strong impacts of agricultural fires (Figure 8b). A possible explanation was
414 that some fire-emitted chromophores were more or less distributed on relatively large particles that
415 would be removed by the inlet of LV but could pass through that of HV. Although these
416 chromophores represented an important contributor to BrC absorption, their influence on BrC mass
417 was likely insignificant, as indicated by the little influence of agricultural fires on the LV-to-HV
418 ratio of BrC mass (Figure S6).

419 Finally, it should be noted that for the species except K^+ and $(b_{abs})_{365}$, their LV-to-HV ratios
420 still showed different patterns of distribution (Figure 7). Analytical uncertainties should be partially
421 responsible, e.g., as indicated by the more significant variations in the LV-to-HV ratios of EC^*
422 compared to those of OC^*. Another likely cause was that the sampling duration of a given LV sample
423 (24 hours) actually did not equal that of the corresponding HV (15 hours), which would result in

https://doi.org/10.5194/egusphere-2025-537
Preprint. Discussion started: 17 March 2025

different LV-to-HV ratios for the species with different diurnal cycles. In summary, many factors could be responsible for the inter-sampler discrepancies shown in Figure 7. Typically, the overall effects of these factors were higher LV-based concentrations than HV, with median LV-to-HV ratios concentrating in a relatively narrow range of 1–1.15. However, this comparability may not always hold. A possible explanation was that the impactor performances were more or less different between the two samplers, thus for specific components such as K^+ and some fire-emitted chromophores, this difference could exert a significant influence on their sampling.

4. Conclusions and implications

For the first time, EC results were compared among different sampling and analytical approaches based on field observations in Northeast China. Two samplers with flow rates of 1.13 m^3/min and 5 L/min were operated together during two distinct seasons, whereas thermal-optical analysis was performed by applying different protocols to both the untreated and extracted filters. Results from different seasons jointly suggested that $EC_{extracted}$ measured by IMPROVE-A (i.e., IMPV) was biased by complex artifacts associated with sulfate. The IMPV-based $EC_{extracted}$ tended to underestimate elemental carbon mass when sulfate was less abundant, whereas overestimations were evident at sufficiently high loadings of sulfate. The turning point for the artifact shifting from an underestimation to overestimation occurred in the sulfate loading range of 10–15 μg/cm^2. Such high sulfate loadings were rarely encountered by the LV samples and thus the corresponding IMPV-based EC typically decreased after the extraction (by ~20%). For the HV samples, their sulfate covered a wide range of ~2–35 μg/cm^2 during winter and in this case, the extraction-induced changes in EC usually varied between –50% and +50% for the IMPV-based results. In addition to the complex sulfate-related artifacts, another problem identified for the IMPV-based $EC_{extracted}$ was

https://doi.org/10.5194/egusphere-2025-537
Preprint. Discussion started: 17 March 2025

that in winter, the corresponding OC/EC ratio exhibited relatively weak or even no association with the SNA/CO ratio, which was used as an indicator for the significance of secondary aerosol production. The NIOSH-based OC/EC occasionally showed acceptable correlation with SNA/CO, but it was never effectively enhanced by agricultural fire emissions. Then the IMPV-based $EC_{untreated}$ (EC^{*}) was recommended, as the corresponding OC/EC could always be reasonably linked to aerosol sources, e.g., secondary aerosol formation in winter and agricultural fire impacts (as reflected by f_{LG}) in spring.

Inter-sampler comparisons were performed for various species that are of broad interest in field observations, including EC^{*}. Although the flow rates differed by more than two orders of magnitude between the two samplers, the LV and HV generally led to comparable measurement results for the majority of the species, with the median LV-to-HV ratios falling within a relatively narrow range of 1–1.15.

This study also raised two points that merit attentions. The first is that the IMPV-based $EC_{untreated}$, which was suggested for investigations on aerosol sources, might overestimate elemental carbon mass under extremely strong impacts of open burning. This problem was attributed to strongly absorbing BrC emitted by agricultural fires with relatively low combustion efficiencies. Although uncommon for the ambient samples in Harbin (a megacity located in a main agricultural region in China), this problem could introduce substantial uncertainties to the emission factors and thus inventories of biomass burning. We suggested that a key step to refine the EC measurement results was to concurrently minimize the inferences from strongly absorbing BrC and scattering components. Methanol extraction followed by water extraction of filter samples was expected to be a practical approach, which was worthy of further evaluations.

https://doi.org/10.5194/egusphere-2025-537
Preprint. Discussion started: 17 March 2025

The second point was that some specific components should be interpreted with caution, even when comparing their measurement results from samplers with the same nominal cut-point. Our observational results indicated that some relatively large particles, if present, could be collected onto the filters of the high-volume $PM_{2.5}$ sampler but would be removed by the inlet of the low-volume one. This problem was attributed to the fact that the inlet performances (e.g., the size-cut curve) could not be exactly the same between the HV and LV $PM_{2.5}$ samplers. Among the various species involved in this study, this problem affected the measurements of K^+ as well as some fire-emitted chromophores in the fine mode. Thus we suggested that the K^+ results derived from different $PM_{2.5}$ samplers may not be directly comparable. In addition, although we could not quantitatively determine the dust contribution to K^+ measured by the high-volume $PM_{2.5}$ sampler, K^+ should be used with caution as a biomass burning tracer for source apportionment studies relying on the HV-based observations.

Data availability. Data are available from the corresponding author upon request (jiumengliu@hit.edu.cn).

Author contributions. YC and JL designed the study and prepared the paper, with inputs from all the co-authors. YZ, ZZ and XC carried out the experiments.

Competing interests. The authors declare that they have no conflict of interest.

Disclaimer. Publisher's note: Copernicus Publications remains neutral with regard to jurisdictional claims made in the text, published maps, institutional affiliations, or any other geographical representation in this paper. While Copernicus Publications makes every effort to include appropriate place names, the final responsibility lies with the authors.

Acknowledgements. The authors thank Zhen-yu Du at the National Research Center for

https://doi.org/10.5194/egusphere-2025-537
Preprint. Discussion started: 17 March 2025

Environmental Analysis and Measurement and Lin-lin Liang at the Chinese Academy of Meteorological Sciences for their help in sample analysis.

Financial support. This research has been supported by the National Natural Science Foundation of China (42222706), the Natural Science Foundation of Heilongjiang Province (YQ2024D011), the State Key Laboratory of Urban Water Resource and Environment (2023DX10) and the Fundamental Research Funds for the Central Universities.

References

Aakko-Saksa, P., Koponen, P., Aurela, M., Vesala, H., Piimäkorpi, P., Murtonen, T., Sippula, O., Koponen, H., Karjalainen, P., Kuittinen, N., Panteliadis, P., Rönkkö, T., and Timonen, H.: Considerations in analysing elemental carbon from marine engine exhaust using residual, distillate and biofuels, ***J. Aerosol Sci.***, 126, 191–204, 2018.

Andela, N., Morton, D. C., Schroeder, W., Chen, Y., Brando, P. M., and Randerson, J. T.: Tracking and classifying Amazon fire events in near real time, ***Sci. Adv.***, 8, eabd2713, 2022.

Andreae, M. O., and Gelencsér, A.: Black carbon or brown carbon? The nature of light-absorbing carbonaceous aerosols, ***Atmos. Chem. Phys.***, 6, 3131–3148, 2006.

Buffaloe, G. M., Lack, D. A., Williams, E. J., Coffman, D., Hayden, K. L., Lerner, B. M., Li, S. M., Nuaaman, I., Massoli, P., Onasch, T. B., Quinn, P. K., and Cappa, C. D.: Black carbon emissions from in-use ships: a California regional assessment, ***Atmos. Chem. Phys.***, 14, 1881–1896, 2014.

Cavalli, F., Viana, M., Yttri, K. E., Genberg, J., and Putaud, J. P.: Toward a standardized thermal-optical protocol for measuring atmospheric organic and elemental carbon: the EUSAAR protocol, ***Atmos. Meas. Tech.***, 3, 79–89, 2010.

Chakrabarty, R. K., Shetty, N. J., Thind, A. S., Beeler, P., Sumlin, B. J., Zhang, C. C., Liu, P., Idrobo, J. C., Adachi, K., Wagner, N. L., Schwarz, J. P., Ahern, A., Sedlacek, A. J., Lambe, A., Daube, C., Lyu, M., Liu, C., Herndon, S., Onasch, T. B., and Mishra, R.: Shortwave absorption by wildfire smoke dominated by dark brown carbon, ***Nat. Geosci.***, 16, 683–688, 2023.

https://doi.org/10.5194/egusphere-2025-537
Preprint. Discussion started: 17 March 2025

516 Chang, X., Zhao, B., Zheng, H. T., Wang, S. X., Cai, S. Y., Guo, F. Q., Gui, P., Huang, G. H., Wu,
517 D., Han, L. C., Xing, J., Man, H. Y., Hu, R. L., Liang, C. R., Xu, Q. C., Qiu, X. H., Ding, D.,
518 Liu, K. Y., Han, R., Robinson, A. L., and Donahue, N. M.: Full-volatility emission framework
519 corrects missing and underestimated secondary organic aerosol sources, ***One Earth***, 5, 403–
520 412, 2022.

521 Chen, P. F., Kang, S. C., Tripathee, L., Ram, K., Rupakheti, M., Panday, A. K., Zhang, Q., Guo, J.
522 M., Wang, X. X., Pu, T., and Li, C. L.: Light absorption properties of elemental carbon (EC)
523 and water-soluble brown carbon (WS-BrC) in the Kathmandu Valley, Nepal: a 5-year study,
524 ***Environ. Pollut.***, 261, 114239, 2020.

525 Cheng, J., Tong, D., Zhang, Q., Liu, Y., Lei, Y., Yan, G., Yan, L., Yu, S., Cui, R. Y., Clarke, L., Geng,
526 G. N., Zheng, B., Zhang, X. Y., Davis, S. J., and He, K. B.: Pathways of China's $PM_{2.5}$ air
527 quality 2015-2060 in the context of carbon neutrality, ***Natl. Sci. Rev.***, 8, nwab078, 2021.

528 Cheng, Y., Cao, X. B., Yu, Q. Q., Liu, J. M., Ma, W. L., Qi, H., Zhang, Q., and He, K. B.: Synergy
529 of multiple drivers leading to severe winter haze pollution in a megacity in Northeast China,
530 ***Atmos. Res.***, 270, 106075, 2022.

531 Cheng, Y., Cao, X. B., Zhu, S. Q., Zhang, Z. Q., Liu, J. M., Zhang, H. L., Zhang, Q., and He, K. B.:
532 Exploring the sources of light-absorbing carbonaceous aerosols by integrating observational
533 and modeling results: insights from Northeast China, ***Atmos. Chem. Phys.***, 24, 9869–9883,
534 2024.

535 Chiappini, L., Verlhac, S., Aujay, R., Maenhaut, W., Putaud, J. P., Sciare, J., Jaffrezo, J. L., Liousse,
536 C., Galy-Lacaux, C., Alleman, L. Y., Panteliadis, P., Leoz, E., and Favez, O.: Clues for a
537 standardised thermal-optical protocol for the assessment of organic and elemental carbon
538 within ambient air particulate matter, ***Atmos. Meas. Tech.***, 7, 1649–1661, 2014

539 Collaud Coen, M., Weingartner, E., Apituley, A., Ceburnis, D., Fierz-Schmidhauser, R., Flentje, H.,
540 Henzing, J. S., Jennings, S. G., Moerman, M., Petzold, A., Schmid, O., and Baltensperger, U.:
541 Minimizing light absorption measurement artifacts of the Aethalometer: evaluation of five
542 correction algorithms, ***Atmos. Meas. Tech.***, 3, 457–474, 2010.

https://doi.org/10.5194/egusphere-2025-537
Preprint. Discussion started: 17 March 2025

543 Costa, V., Bacco, D., Castellazzi, S., Ricciardelli, I., Vecchietti, R., Zigola, C., and Pietrogrande, M.
544 C.: Characteristics of carbonaceous aerosols in Emilia-Romagna (Northern Italy) based on two
545 fall/winter field campaigns, ***Atmos. Res.***, 167, 100–107, 2016.

546 Dao, X., Lin, Y. C., Cao, F., Di, S. Y., Hong, Y. H., Xing, G. H., Li, J. J., Fu, P. Q., and Zhang, Y. L.:
547 Introduction to the national aerosol chemical composition monitoring network of China:
548 objectives, current status, and outlook, ***Bull. Am. Meteorol. Soc.***, 100, ES337–ES351, 2019.

549 Eckhardt, S., Pisso, I., Evangeliou, N., Zwaaftink, C. G., Plach, A., McConnell, J. R., Sigl, M.,
550 Ruppel, M., Zdanowicz, C., Lim, S., Chellman, N., Opel, T., Meyer, H., Steffensen, J. P.,
551 Schwikowski, M., and Stohl, A.: Revised historical Northern Hemisphere black carbon
552 emissions based on inverse modeling of ice core records, ***Nat. Commun.***, 14, 271, 2023.

553 Fuzzi, S., Baltensperger, U., Carslaw, K., Decesari, S., van der Gon, H. D., Facchini, M. C., Fowler,
554 D., Koren, I., Langford, B., Lohmann, U., Nemitz, E., Pandis, S., Riipinen, I., Rudich, Y.,
555 Schaap, M., Slowik, J. G., Spracklen, D. V., Vignati, E., Wild, M., Williams, M., and Gilardoni,
556 S.: Particulate matter, air quality and climate: lessons learned and future needs, ***Atmos. Chem.***
557 ***Phys.***, 15, 8217–8299, 2015.

558 Garofalo, L. A., Pothier, M. A., Levin, E. J. T., Campos, T., Kreidenweis, S. M., and Farmer, D. K.:
559 Emission and evolution of submicron organic aerosol in smoke from wildfires in the Western
560 United States, ***ACS Earth Space Chem.***, 3, 1237–1247, 2019.

561 Gao, C. Y., Heald, C. L., Katich, J. M., Luo, G., and Yu, F. Q.: Remote aerosol simulated during the
562 Atmospheric Tomography (ATom) campaign and implications for aerosol lifetime, ***J. Geophys.***
563 ***Res. Atmos.***, 127, e2022JD036524, 2022.

564 Gao, S., Hegg, D. A., Hobbs, P. V., Kirchstetter, T. W., Magi, B. I., and Sadilek, M.: Water-soluble
565 organic components in aerosols associated with savanna fires in southern Africa: identification,
566 evolution, and distribution, ***J. Geophys. Res.***, 108, 8491, 2003.

567 Giannoni, M., Calzolai, G., Chiari,M., Cincinelli, A., Lucarelli, F., Martellini, T., and Nava, S.: A
568 comparison between thermal-optical transmittance elemental carbon measured by different
569 protocols in $PM_{2.5}$ samples, ***Sci. Total Environ.***, 571, 195–205, 2016.

https://doi.org/10.5194/egusphere-2025-537
Preprint. Discussion started: 17 March 2025

570 Gkatzelis, G. I., Coggon, M. M., Stockwell, C. E., Hornbrook, R. S., Allen, H., Apel, E. C., Bela,
571 M. M., Blake, D. R., Bourgeois, I., Brown, S. S., Campuzano-Jost, P., St. Clair, J. M., Crawford,
572 J. H., Crounse, J. D., Day, D. A., DiGangi, J. P., Diskin, G. S., Fried, A., Gilman, J. B., Guo,
573 H., Hair, J. W., Halliday, H. S., Hanisco, T. F., Hannun, R., Hills, A., Huey, L. G., Jimenez, J.
574 L., Katich, J. M., Lamplugh, A., Lee, Y. R., Liao, J., Lindaas, J., McKeen, S. A., Mikoviny, T.,
575 Nault, B. A., Neuman, J. A., Nowak, J. B., Pagonis, D., Peischl, J., Perring, A. E., Piel, F.,
576 Rickly, P. S., Robinson, M. A., Rollins, A. W., Ryerson, T. B., Schueneman, M. K., Schwantes,
577 R. H., Schwarz, J. P., Sekimoto, K., Selimovic, V., Shingler, T., Tanner, D. J., Tomsche, L.,
578 Vasquez, K. T., Veres, P. R., Washenfelder, R., Weibring, P., Wennberg, P. O., Wisthaler, A.,
579 Wolfe, G. M., Womack, C. C., Xu, L., Ball, K., Yokelson, R. J., and Warneke, C.:
580 Parameterizations of US wildfire and prescribed fire emission ratios and emission factors based
581 on FIREX-AQ aircraft measurements, ***Atmos. Chem. Phys.***, 24, 929–956, 2024.

582 Hand, J. L., Prenni, A. J., Raffuse, S. M., Hyslop, N. P., Malm, W. C., and Schichtel, B. A.: Spatial
583 and seasonal variability of remote and urban speciated fine particulate matter in the United
584 States, ***J. Geophys. Res. Atmos.***, 129, e2024JD042579, 2024

585 Hecobian, A., Zhang, X., Zheng, M., Frank, N., Edgerton, E. S., and Weber, R. J.: Water-soluble
586 organic aerosol material and the light-absorption characteristics of aqueous extracts measured
587 over the Southeastern United States, ***Atmos. Chem. Phys.***, 10, 5965–5977, 2010.

588 Hu, Z. F., Kang, S. C., Xu, J. Z., Zhang, C., Li, X. F., Yan, F. P., Zhang, Y. L., Chen, P. F., and Li, C.
589 L.: Significant overestimation of black carbon concentration caused by high organic carbon in
590 aerosols of the Tibetan Plateau, ***Atmos. Environ.***, 294, 119486, 2023.

591 Knox, A., Evans, G. J., Brook, J. R., Yao, X., Jeong, C. H., Godri, K. J., Sabaliauskas, K., and
592 Slowik, J. G.: Mass absorption cross-section of ambient black carbon aerosol in relation to
593 chemical age, ***Aerosol Sci. Technol.***, 43, 522–532, 2009.

594 Laborde, M., Schnaiter, M., Linke, C., Saathoff, H., Naumann, K. H., Möhler, O., Berlenz, S.,
595 Wagner, U., Taylor, J. W., Liu, D., Flynn, M., Allan, J. D., Coe, H., Heimerl, K., Dahlkötter, F.,
596 Weinzierl, B., Wollny, A. G., Zanatta, M., Cozic, J., Laj, P., Hitzenberger, R., Schwarz, J. P.,
597 and Gysel, M.: Single Particle Soot Photometer intercomparison at the AIDA chamber, ***Atmos.***

https://doi.org/10.5194/egusphere-2025-537
Preprint. Discussion started: 17 March 2025

Meas. Tech., 5, 3077–3097, 2012.

Lack, D. A., Moosmüller, H., McMeeking, G. R., Chakrabarty, R. K., and Baumgardner, D.: Characterizing elemental, equivalent black, and refractory black carbon aerosol particles: a review of techniques, their limitations and uncertainties, ***Anal. Bioanal. Chem.***, 406, 99–122, 2014.

Lappi, M. K., and Ristimäki, J. M.: Evaluation of thermal optical analysis method of elemental carbon for marine fuel exhaust, ***J. Air Waste Manage. Assoc.***, 67, 1298–1318, 2017.

Li, H. Y., Lamb, K. D., Schwarz, J. P., Selimovic, V., Yokelson, R. J., McMeeking, G. R., and May, A. A.: Inter-comparison of black carbon measurement methods for simulated open biomass burning emissions, ***Atmos. Environ.***, 206, 156–169, 2019.

Li, J., Carlson, B. E., Yung, Y. L., Lv, D. R., Hansen, J., Penner, J. E., Liao, H., Ramaswamy, V., Kahn, R. A., Zhang, P., Dubovik, O., Ding, A. J., Lacis, A. A., Zhang, L., and Dong, Y. M.: Scattering and absorbing aerosols in the climate system, ***Nat. Rev. Earth Environ.***, 3, 363–379, 2022.

Liu J. M., Du Z. Y., Liang L. L., Yu Q. Q., Shen G. F., Ma Y. L., Zheng M., Cheng Y., and He K. B.: Uncertainties in thermal-optical measurements of black carbon: insights from source and ambient samples, ***Sci. Total Environ.***, 656, 239–249, 2019.

Liu, J. M., Wang, P. F., Zhang, H. L., Du, Z. Y., Zheng, B., Yu, Q. Q., Zheng, G. J., Ma, Y. L., Zheng, M., Cheng, Y., Zhang, Q., and He, K. B.: Integration of field observation and air quality modeling to characterize Beijing aerosol in different seasons, ***Chemosphere***, 242, 125195, 2020.

Liu, S. G., Geng, G. N., Xiao, Q. Y., Zheng, Y. X., Liu, X. D., Cheng, J., and Zhang, Q.: Tracking daily concentrations of $PM_{2.5}$ chemical composition in China since 2000, ***Environ. Sci. Technol.***, 56, 16517–16527, 2022.

Liu, X. X., Zhang, Y., Huey, L. G., Yokelson, R. J., Wang, Y., Jimenez, J. L., Campuzano-Jost, P., Beyersdorf, A. J., Blake, D. R., Choi, Y., St Clair, J. M., Crounse, J. D., Day, D. A., Diskin, G. S., Fried, A., Hall, S. R., Hanisco, T. F., King, L. E., Meinardi, S., Mikoviny, T., Palm, B. B.,

https://doi.org/10.5194/egusphere-2025-537
Preprint. Discussion started: 17 March 2025

Peischl, J., Perring, A. E., Pollack, I. B., Ryerson, T. B., Sachse, G., Schwarz, J. P., Simpson, I. J., Tanner, D. J., Thornhill, K. L., Ullmann, K., Weber, R. J., Wennberg, P. O., Wisthaler, A., Wolfe, G. M., and Ziemba, L. D.: Agricultural fires in the southeastern U.S. during SEAC^{4}RS: Emissions of trace gases and particles and evolution of ozone, reactive nitrogen, and organic aerosol, ***J. Geophys. Res. Atmos.***, 121, 7383–7414, 2016.

Petzold, A., Ogren, J. A., Fiebig, M., Laj, P., Li, S. M., Baltensperger, U., Holzer-Popp, T., Kinne, S., Pappalardo, G., Sugimoto, N., Wehrli, C., Wiedensohler, A., and Zhang, X. Y.: Recommendations for reporting "black carbon" measurements, ***Atmos. Chem. Phys.***, 13, 8365–8379, 2013.

Petzold, A., Schloesser, H., Sheridan, P. J., Arnott, W. P., Ogren, J. A., and Virkkula, A.: Evaluation of multiangle absorption photometry for measuring aerosol light absorption, ***Aerosol Sci. Technol.***, 39, 40–51, 2005.

Philip, S., Martin, R., van Donkelaar, A., Lo, J. W. H., Wang, Y. X., Chen, D., Zhang, L., Kasibhatla, P. S., Wang, S. W., Zhang, Q., Lu, Z., Streets, D. G., Bittman, S., and MacDonald, D. J.: Global chemical composition of ambient fine particulate matter for exposure assessment, ***Environ. Sci. Technol.***, 48, 13060–13068, 2014.

Piazzalunga, A., Bernardoni, V., Fermo, P., Valli, G., and Vecchi, R.: Technical note: On the effect of water-soluble compounds removal on EC quantification by TOT analysis in urban aerosol samples, ***Atmos. Chem. Phys.***, 11, 10193–10203, 2011.

Pileci, R. E., Modini, R. L., Bertò, M., Yuan, J., Corbin, J. C., Marinoni, A., Henzing, B., Moerman, M. M., Putaud, J. P., Spindler, G., Wehner, B., Müller, T., Tuch, T., Trentini, A., Zanatta, M., Baltensperger, U., and Gysel-Beer, M.: Comparison of co-located refractory black carbon (rBC) and elemental carbon (EC) mass concentration measurements during field campaigns at several European sites, ***Atmos. Meas. Tech.***, 14, 1379–1403, 2021.

Pöschl, U.: Atmospheric aerosols: composition, transformation, climate and health effects, ***Angew. Chem. Int. Ed.***, 44, 7520–7540, 2005.

Putaud, J. P., Van Dingenen, R., Alastuey, A., Bauer, H., Birmili, W., Cyrys, J., Flentje, H., Fuzzi,

https://doi.org/10.5194/egusphere-2025-537
Preprint. Discussion started: 17 March 2025

652 S., Gehrig, R., Hansson, H. C., Harrison, R. M., Herrmann, H., Hitzenberger, R., Hüglin, C.,
653 Jones, A. M., Kasper-Giebl, A., Kiss, G., Kousa, A., Kuhlbusch, T. A. J., Löschau, G.,
654 Maenhaut, W., Molnar, A., Moreno, T., Pekkanen, J., Perrino, C., Pitz, M., Puxbaum, H.,
655 Querol, X., Rodriguez, S., Salma, I., Schwarz, J., Smolik, J., Schneider, J., Spindler, G., ten
656 Brink, H., Tursic, J., Viana, M., Wiedensohler, A., and Raes, F.: A European aerosol
657 phenomenology-3: Physical and chemical characteristics of particulate matter from 60 rural,
658 urban, and kerbside sites across Europe, ***Atmos. Environ.***, 44, 1308–1320, 2020.

659 Qin, Y. M., Tan, H. B., Li, Y. J., Li, Z. J., Schurman, M. I., Liu, L., Wu, C., and Chan, C. K.:
660 Chemical characteristics of brown carbon in atmospheric particles at a suburban site near
661 Guangzhou, China, ***Atmos. Chem. Phys.***, 18, 16409–16418, 2018.

662 Samset, B. H., Myhre, G., Herber, A., Kondo, Y., Li, S. M., Moteki, N., Koike, M., Oshima, N.,
663 Schwarz, J. P., Balkanski, Y., Bauer, S. E., Bellouin, N., Berntsen, T. K., Bian, H., Chin, M.,
664 Diehl, T., Easter, R. C., Ghan, S. J., Iversen, T., Kirkevåg, A., Lamarque, J. F., Lin, G., Liu, X.,
665 Penner, J. E., Schulz, M., Seland, Ø., Skeie, R. B., Stier, P., Takemura, T., Tsigaridis, K., and
666 Zhang, K.: Modelled black carbon radiative forcing and atmospheric lifetime in AeroCom
667 Phase II constrained by aircraft observations, ***Atmos. Chem. Phys.***, 14, 12465–12477, 2014.

668 Shen, G. F., Chen, Y. C., Wei, S. Y., Fu, X. F., Zhu, Y., and Tao, S.: Mass absorption efficiency of
669 elemental carbon for source samples from residential biomass and coal combustions, ***Atmos.***
670 ***Environ.***, 79, 79–84, 2013

671 Subramanian, R., Khlystov, A. Y., and Robinson, A. L.: Effect of peak inert-mode temperature on
672 elemental carbon measured using thermal-optical analysis, ***Aerosol Sci. Technol.***, 40, 763–780,
673 2006.

674 Sullivan, A. P., Guo, H., Schroder, J. C., Campuzano-Jost, P., Jimenez, J. L., Campos, T., Shah, V.,
675 Jaeglé, L., Lee, B. H., Lopez-Hilfiker, F. D., Thornton, J. A., Brown, S. S., and Weber, R. J.:
676 Biomass burning markers and residential burning in the WINTER aircraft campaign, ***J.***
677 ***Geophys. Res. Atmos.***, 124, 1846–1861, 2019.

678 Tinorua, S., Denjean, C., Nabat, P., Pont, V., Arnaud, M., Bourrianne, T., Dias Alves, M., and
679 Gardrat, E.: A 2-year intercomparison of three methods for measuring black carbon

https://doi.org/10.5194/egusphere-2025-537
Preprint. Discussion started: 17 March 2025

concentration at a high-altitude research station in Europe, ***Atmos. Meas. Tech.***, 17, 3897–3915, 2024.

von Schneidemesser, E., Monks, P. S., Allan, J. D., Bruhwiler, L., Forster, P., Fowler, D., Lauer, A., Morgan, W. T., Paasonen, P., Righi, M., Sindelarova, K., and Sutton, M. A.: Chemistry and the linkages between air quality and climate change, ***Chem. Rev.***, 115, 3856–3897, 2015.

Wang, G. H., Cheng, C. L., Huang, Y., Tao, J., Ren, Y. Q., Wu, F., Meng, J. J., Li, J. J., Cheng, Y. T., Cao, J. J., Liu, S. X., Zhang, T., Zhang, R., and Chen, Y. B.: Evolution of aerosol chemistry in Xi'an, inland China, during the dust storm period of 2013 – Part 1: Sources, chemical forms and formation mechanisms of nitrate and sulfate, ***Atmos. Chem. Phys.***, 14, 11571–11585, 2014a.

Wang, R., Tao, S., Balkanski, Y., Ciais, P., Boucher, O., Liu, J. F., Piao, S. L., Shen, H. Z., Vuolo, M. R., Valari, M., Chen, H., Chen, Y. C., Cozic, A., Huang, Y., Li, B. G., Li, W., Shen, G. F., Wang, B., and Zhang, Y. Y.: Exposure to ambient black carbon derived from a unique inventory and high-resolution model, ***Proc. Natl. Acad. Sci. U. S. A.***, 111, 2459–2463, 2014b.

Wang, X., Heald, C. L., Liu, J. M., Weber, R. J., Campuzano-Jost, P., Jimenez, J. L., Schwarz, J. P., and Perring, A. E.: Exploring the observational constraints on the simulation of brown carbon, ***Atmos. Chem. Phys.***, 18, 635–653, 2018.

Wei, J., Li, Z. Q., Lyapustin, A., Wang, J., Dubovik, O., Schwartz, J., Sun, L., Li, C., Liu, S., and Zhu, T.: First close insight into global daily gapless 1 km $PM_{2.5}$ pollution, variability, and health impact, ***Nat. Commun.***, 14, 8349, 2023.

Xiao, Q. Y., Geng, G. N., Xue, T., Liu, S. G., Cai, C. L., He, K. B., and Zhang, Q.: Tracking $PM_{2.5}$ and O_3 Pollution and the related health burden in China 2013-2020, ***Environ. Sci. Technol.***, 56, 6922–6932, 2022.

Yang, H., and Yu, J. Z.: Uncertainties in charring correction in the analysis of elemental and organic carbon in atmospheric particles by thermal/optical methods, ***Environ. Sci. Technol.***, 36, 5199–5204, 2002.

Yu, J. Z., Xu, J. H., and Yang, H.: Charring characteristics of atmospheric organic particulate matter

https://doi.org/10.5194/egusphere-2025-537
Preprint. Discussion started: 17 March 2025

in thermal analysis, ***Environ. Sci. Technol.***, 36, 754–761, 2002.

Zheng, G. J., Duan, F. K., Su, H., Ma, Y. L., Cheng, Y., Zheng, B., Zhang, Q., Huang, T., Kimoto, T., Chang, D., Pöschl, U., Cheng, Y. F., and He, K. B.: Exploring the severe winter haze in Beijing: the impact of synoptic weather, regional transport and heterogeneous reactions, ***Atmos. Chem. Phys.***, 15, 2969–2983, 2015.

Zhong, Q. R., Schutgens, N., van der Werf, G. R., Takemura, T., van Noije, T., Mielonen, T., Checa-Garcia, R., Lohmann, U., Kirkevåg, A., Oliviè, D. J. L., Kokkola, H., Matsui, H., Kipling, Z., Ginoux, P., Le Sager, P., Rémy, S., Bian, H. S., Chin, M., Zhang, K., Bauer, S. E., and Tsigaridis, K.: Threefold reduction of modeled uncertainty in direct radiative effects over biomass burning regions by constraining absorbing aerosols, ***Sci. Adv.***, 9, eadi3568, 2023.